Polymer 51 (2010) 2417–2425

Contents lists available at ScienceDirect

Polymer

journal homepage: www.elsevier.com/locate/polymer

Eutectic melting behavior of polyamide 10,T-co-6,T and 12,T-co-6,T copolyterephthalamides

Theodore F. Novitsky [a], Christopher A. Lange [a], Lon J. Mathias [a,*], Scott Osborn [b], Roger Ayotte [b], Steven Manning [b]

[a] The University of Southern Mississippi, 118 College Drive, Hattiesburg, MS 39402, USA
[b] Ascend Performance Materials, 3000 Old Chemstrand Road, Cantonment, FL 32533, USA

ARTICLE INFO

Article history:
Received 29 January 2010
Received in revised form
19 March 2010
Accepted 25 March 2010
Available online 31 March 2010

Keywords:
Copolyamide
Eutectic melting temperature
NMR

ABSTRACT

Semi-aromatic polyterephthalamides 10,T and 12,T were synthesized with 0–60 wt-% PA-6,T comonomer by a melt polycondensation process. Molecular weights of the copolymers ranged from 12,000 to 27,000 g/mol and all produced tough melt-pressed films. The substituted aromatic carbon of the ^{13}C NMR spectra revealed that comonomer sequences are statistical; e.g., 50:50 wt-% PA-12,T-co-6,T copolymer had 12,T-12,T:12,T-6,T:6,T-6,T sequence ratios of approximately 1:2:1. Copolymers of both PA-10,T and 12,T exhibited a eutectic melting point at 30 wt-% PA-6,T, with melting points decreasing linearly from 315 and 292 °C to minima of 280 and 272 °C, respectively. Melting enthalpies showed similar minima at ca. 35 wt-% PA-6,T. WAXD and DMA were used to further characterize the eutectic behavior, and a comprehensive analysis of PA-6,T copolymer melting behavior is given.

1. Introduction

Semi-aromatic polyamides combine the high melting temperatures and heat resistance of wholly aromatic polyamides (e.g., Kevlar poly p-phenylene terephthalamide) with the melt processability of aliphatic polyamides such as nylon 6 and 6,6. Much research has focused on semi-aromatic polyamides synthesized using aliphatic diamines and terephthalic acid [1,2]. With short aliphatic diamines (2–7 CH_2's), melting temperatures surpass the thermal decomposition temperature of polyamides, thus making melt processing impractical. For example, the melting points of PA-4,T and PA-6,T are 430 and 370 °C, respectively [3]. Increasing the length of the aliphatic diamine lowers the melting point into a processable range. For instance, the melting points of PA-9,T, PA-10,T, PA-12,T [2] and PA-18,T [4] are approximately 309, 315, 295 and 245 °C, respectively. More important for high temperature applications, semi-aromatic polyamides have glass transition temperatures ranging from 100 to 140 °C (as observed by DSC).

Comonomers are commonly used in semi-aromatic polyamides to alter properties such as melting temperature, processability, and optical clarity [1]. Copolyamide crystallinity is dependent on degree of symmetry, the distance between amide bonds and amide bond orientation (odd–even effect). These effects are characterized by plotting copolymer melting temperature and enthalpies versus composition. If melting temperatures do not display a local minimum as a function of composition, the comonomers are said to be isomorphous, as is seen for adipic acid and terephthalic acid in nylon 6,6-co-6,T and 4,6-co-4,T copolymers [5–8]. Such co-crystallization is due to the similar lengths between amide groups of adipic acid and terephthalic acid units, which allow incorporation into the same crystal structure while having no change in crystal lattice dimensions. Co-crystalline copolymers also display no apparent decrease in crystallinity. Alternatively, when a local minimum, or eutectic point, is observed, the comonomers are not co-crystalline and thus do not fit into the same crystalline lattice: the comonomer acts as an impurity which decreases the size, perfection, and melting point of the formed crystals. For example, when copolymerized with the crystalline PA-6,T, the amorphous PA-6, I-[poly(hexamethylene isophthalamide)] displays a drastic drop in melting temperature occurs at 50 wt-%, rendering their copolymers amorphous [9]. However, when two crystalline polymers are copolymerized, isodimorphism is known to occur, characterized by a change in crystal lattice dimensions at the eutectic point [10]. In this case, the comonomer is incorporated into a crystal structure different than its own. The degree of melting point depression and amount of crystallinity at the eutectic point are a function of structural similarity of the comonomer repeating units.

Research reported on PA-10,T copolymers has been limited to copolymerizations involving caprolactam and adipic acid [6,11]. It

* Corresponding author. Tel.: +1 (601) 266 4873; fax: +1 (601) 266 5504.
E-mail address: lon.mathias@usm.edu (L.J. Mathias).

0032-3861/$ – see front matter © 2010 Elsevier Ltd. All rights reserved.
doi:10.1016/j.polymer.2010.03.045

has been demonstrated that adipic acid and terephthalic acid co-crystallize when polymerized with decamethylene diamine, resulting in melting point versus composition trends similar to that of the nylon 6,6-co-6,T series. No literature currently exists covering the copolymerization of PA-10,T or 12,T with other linear diamines. A single reference describes semi-aromatic copolyamides synthesized using terephthalic acid and a combination of linear aliphatic diamines [12]. It was reported that copolyamides of PA-4,T and 6,T display a minimum of melting temperature with composition, but maintain some level of crystallinity throughout all compositions despite the two monomers being non-isomorphic.

It is the goal of this study to determine the effect of the distance between amide bonds on the melting behavior of semi-aromatic copolyterephthalamides by changing the diamine length while keeping amide orientation fixed by using solely even diamines. PA-10,T-co-6,T and PA-12,T-co-6,T copolymers were synthesized by melt condensation polymerization of mixed diamine/terephthalic acid salts. Polymers were characterized using high resolution ^{13}C NMR spectroscopy for composition analysis, and intrinsic viscosity for molecular weight estimation. The effect of the PA-6,T comonomer on melting temperature, crystal type, and degree of crystallinity was studied by differential scanning calorimetry, wide-angle x-ray diffraction, and dynamic mechanical analysis.

2. Experimental

2.1. Materials

Terephthalic acid, 1,10-diaminodecane, 1,12-diaminododecane, and 1,6-diaminohexane (HMDA) were purchased from Aldrich. Terephthalic acid and 1,6-diaminohexane were used as received. 1,10-Diaminodecane, and 1,12-diaminododecane were sublimed at 70 °C and dried at room temperature under vacuum before use. N, N-dimethylacetamide (DMAc) and triethylamine were distilled from barium oxide onto molecular sieves before use. Concentrated sulfuric acid (96%) for viscosity measurements was purchased from Aldrich and used as received. Solutia provided 6,T salt, siloxane antifoam, and a commercial antioxidant.

2.2. Laboratory synthesis of polyamide (n,T) salt

Into a 2 L beaker were added 1 L of deionized water, 1,10-diaminodecane (49.5 g, 0.287 mol) and terephthalic acid (42.3 g, 0.285 mol), and the slurry that formed was heated to a boil. Additional water was added and brought to boil to yield a supersaturated, clear salt solution. The hot salt solution was then added to a 2 L beaker containing 500 mL of reagent alcohol and allowed to cool to room temperature, followed by cooling in a freezer. The precipitate was then filtered and washed with reagent alcohol. The resulting 10,T salt was obtained in near-quantitative yield (95%). PA-12,T salt was prepared in a similar manner. All terephthalic acid salts were precipitated from water into reagent alcohol and dried before use. PA-12,T, 10,T, and 6,T salt melting temperatures were 271.9, 271.6, and 281 °C, respectively, with melting enthalpies between 430 and 450 J/g.

2.3. Synthesis

2.3.1. Melt condensation of polyamide (n,T) and copolymers

Copolymers were synthesized from their corresponding diamine/terephthalic acid salts as shown in Fig. 1. Polyamide (*n*,T) salt, 3 mol-% excess diamine, and 0.5 wt-% antioxidant were weighed and mixed with a mortar and pestle. The solid mixture was then added to a test tube and approximately 50 wt-% deionized water was added to create a slurry. Twelve such test tubes were

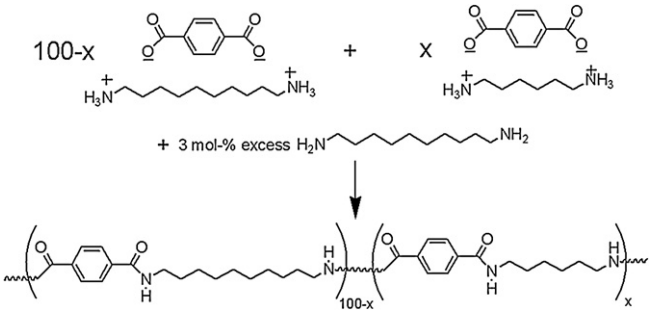

Fig. 1. Synthetic scheme of PA-10,T-co-6,T copolymers, where $x = 0–60$ wt-%.

loaded into a Parr reactor equipped with a test tube holder, which was then sealed and purged with nitrogen. The reactor was surrounded by insulation to improve temperature control. Nitrogen pressure was controlled manually and measured by a gauge on the reactor head.

The melt condensation polymerization was performed in three stages involving water boiling, high pressure, and final hold stage (Fig. 2). Heating steps were programmed into the reactor controller unit and monitored with a thermocouple placed in one of the test tubes. Duration and pressure of each stage were determined by measured temperature of the reaction vessel. The boiling stage ensures homogenization of the reaction mixture, with little polymerization. With approximately 125 kPa nitrogen pressure and a 190 °C set point, the sample temperature remained at 125 °C until all water evaporated. At the completion of boiling and a sudden rise of temperature, the pressure was increased to 1724 kPa to mitigate the loss of diamine throughout this initial stage of the polymerization, and the heater set point was changed to 290 °C. When the reaction temperature reached 280 °C, the pressure was released and the temperature allowed to rise and hold at 310–315 °C for 15 min while maintaining a nitrogen purge.

Initially, higher polymerization temperatures and hold times were used, but this process often resulted in polymers that were neither soluble in sulfuric acid, nor amendable to compression molding. Dimerization of diamines to form crosslinkable triamine species is well known to occur at high reaction temperatures. In order to mitigate this side reaction, a lower maximum temperature (315 rather than 330 °C) and polymerization time (15 rather than 30 min) were used. This resulted in homo- and copolymers that were soluble in both sulfuric and dichloroacetic acid, and were suitable for compression molding into films for testing.

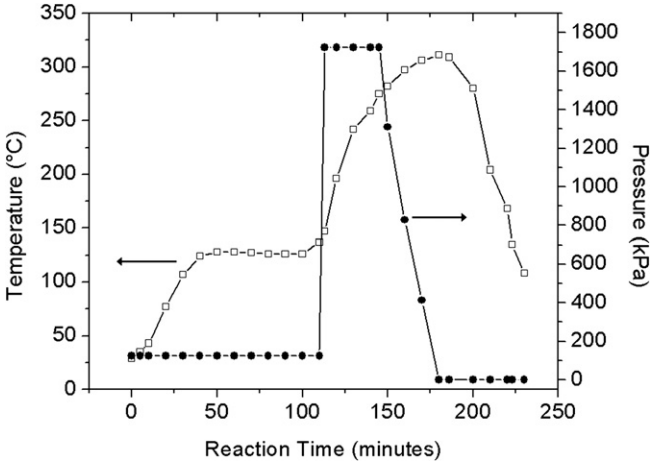

Fig. 2. Melt condensation polymerization temperature and pressure profiles.

2.3.2. Solution polymerization of polyamide 6,T (PA-6,T)

HMDA (10.98 g, 0.095 mol) and triethylamine (27 mL, 0.194 mol) were dissolved in 230 mL of DMAc and added to a Waring blender equipped with a glass container. The blender was turned on high and 60 mL of DMAc containing terephthaloyl chloride (19 g, 0.094 mol) was added as quickly as possible. A white precipitate immediately formed, followed by a large increase in viscosity. After 5 min, blending contents were filtered and the precipitate obtained washed with acetone followed by water, giving PA-6,T (20.7 g, 90%).

2.4. Sample preparation

Solid polymers obtained from the test tubes were immersed in liquid nitrogen for approximately 10 min and then ground using a Waring blender with a stainless steel mixing jar. The samples were then dried at 80 °C under vacuum for 24 h, and stored in a desiccator until further characterization. Dried samples were compression molded into 0.8 or 0.3 mm films at a temperature approximately 10–20 °C above the melting temperature of the polymer as determined by DSC. The pellets were placed between two woven Teflon sheets and held at this temperature between two Carner press hot plates for 3 min with no pressure and then for 2 min under a pressure of 2700 kPa. Hot plates were then taken from the press and immersed in a room temperature water bath. For a higher rate of cooling, films were removed from the hot plates and placed underneath a room temperature steel plate. Films were dried at 80 °C under vacuum for 12 h. Annealing was performed at 200 °C for 12 h under vacuum.

2.5. Characterization

2.5.1. Nuclear magnetic resonance spectroscopy (NMR)

Solutions for NMR analysis having a 10 wt-% polymer concentration were prepared using a 3:1 volume ratio of hexafluoroisopropanol (HFIP) to $CDCl_3$. Samples were first dissolved in HFIP, followed by addition of $CDCl_3$. Solution ^{13}C NMR spectra were collected on a Varian ^{UNITY}INOVA NMR spectrometer operating at a frequency of 125.7 MHz. Routine acquisitions at 25 °C involved a 1.3 s acquisition time, a 45° pulse width of 2.9 μs, and a 1 s recycle delay. The number of accumulated transients ranged from 15,000 to 30,000, requiring 12–24 h collection times. Raw data were zero-filled up to 256k points and filtered with 1 Hz of line broadening prior to application of Fourier transformation. Baselines were corrected using a 10th order polynomial.

2.5.2. Viscometry

Solutions containing 0.5 g/dL of polymer in concentrated sulfuric acid were prepared by adding 0.25 g of polymer and 25 mL of concentrated sulfuric acid into a 50 mL flask. After 12 h of mixing via magnetic stirring, the solutions were diluted with an additional 25 mL of sulfuric acid, and stirring continued for another 12 h. Solutions were visually inspected for gel particles, and passed through a funnel packed with glass fiber if gel was present. Measurements were obtained using a Cannon viscometer in a 25 °C controlled water bath. The viscometer was washed with sulfuric acid and a portion of the next sample to be tested before measurements were recorded. Flow times were an average of three values that agreed within ±0.2 s. Flow times of concentrated sulfuric acid and each of the polymer solutions were used to calculate the specific and relative viscosities. Single point intrinsic viscosities were then determined using the Solomon and Ciuta relationship:

$$[\eta] = \left[2\left(\eta_{sp} - \ln(\eta_{rel})\right)^{1/2}\right]\Big/C$$

where, η_{sp} is the specific viscosity, η_{rel} is the relative viscosity, and C is the concentration [13].

2.5.3. Differential scanning calorimetry (DSC)

Polymer melting temperatures were obtained with a TA Instruments 2920 DSC. Scans were taken at a heating rate of 10 °C/min. Data from both the first and second-heating scans were collected. Samples were heated approximately 10–20 °C above their melting temperature, air cooled to room temperature, and heated a second time to 350 °C.

2.5.4. Wide-angle x-ray scattering (WAXD)

Diffraction patterns were collected on a Rigaku Ultima II x-ray diffractometer. Data were collected from 3 to 40° 2θ at a rate of 2°/min. Samples were annealed at 100 °C for 12–24 h prior to analysis to achieve maximum attainable crystallinity.

2.5.5. Dynamic mechanical analysis (DMA)

Tensile mode DMA data were obtained using a Thermal Analysis Q800 series instrument. Samples of 0.8 mm thickness were prepared by melt pressing, followed by annealing and drying at 200 °C prior to testing. Data were collected from 30 to 250 °C at a heating rate of 2 °C/min with a 20 um amplitude, 0.05 N preload force, and 125% force track.

3. Results

3.1. Intrinsic viscosity and molecular weight

In studies published separately, it was found that PA-12,T samples synthesized with 1 and 3 mol-% excess 1,12-diaminododecane had the lowest total end group concentration, the most balanced acid/amine end groups, and the highest molecular weights, using these melt polymerization conditions [14]. In order to obtain suitable molecular weights for copolymer analysis, 3 mol-% excess deca- or dodecamethylene diamine was added to each reaction. Single point intrinsic viscosities (IV) were determined to estimate the relative number average molecular weights between copolymer samples. IV values for several of the copolymers studied are given in Table 1.

Number average molecular weights for PA-12,T-co-6,T and PA-10,T-co-6,T copolymers were estimated from Mark–Houwink constants developed for PA-12,T homopolymer. Assuming that the solution properties of PA-10,T, 12,T and 6,T are similar, an estimate of M_n for the copolymers was determined using the equation;

$$[\eta] = 0.000558(\mathrm{dL/g})(M_n)\text{^}(0.81)$$

Note that these constants were developed using single point IV values, and this relationship is only applicable for 0.5 g/dL concentrations dissolved in 96% concentrated H_2SO_4 at 25 °C [14]. K and a values were developed from PA-12,T with NMR calculated M_n, and therefore, M_n instead of M_v values are reported.

Table 1
Intrinsic viscosities, estimated M_n values, and 1st heating DSC melt temperatures of homo- and copolymers.

PA-*n*,T-co-6,T (wt-%)	IV	M_n[a] (g/mol)	Tm (°C)
PA-10,T			
100:0	1.68	19,700	327
85:15	1.41	15,900	316
70:30	1.26	13,800	283
50:50	1.68	19,700	324
PA-12,T			
100:0	1.14	12,200	295
85:15	1.21	13,100	287
70:30	1.24	13,500	274
50:50	2.17	27,000	328

[a] $K = 0.000558$ dL/g and $\alpha = 0.81$ in 96% H_2SO_4 at 25 °C.

There are two main effects that create M_n differences in the copolymers: differential diamine volatility and the physical state of the polymer during the reaction. Excess diamine is required in order to maintain balanced stoichiometry. The amount of excess needed is a function of the volatility of the diamine during the polymerization and the polymerization conditions used. Since, hexa-, deca-, and dodecamethylene diamine have different melting points and vapor pressures, using a constant 3 mol-% excess diamine for all copolymer compositions will not result in the same stoichiometric balance under identical polymerization conditions. For example, PA-12,T, 85:15 and 70:30 PA-12,T-co-6,T had intrinsic viscosities of 1.14, 1.21, and 1.24, respectively. Increasing the amount of PA-6,T comonomer has a greater impact on stoichiometric imbalance, because a higher fraction of the more volatile HMDA (compared to deca- and dodecamethylene diamine) is present. If equal molecular weights were desired, the amount of excess diamine would need to be increased corresponding to the amount of PA-6,T comonomer present in order to compensate for these differences in volatility of the two diamine monomers.

Another cause of molecular weight variation is the physical state of the polymer during the reaction, as determined by the relationship between the crystalline melting temperature of the polymer and the maximum reaction temperature. Table 1 lists the DSC melting temperatures of several of the copolymers. The 1st heating DSC data are related to the crystalline state of the polymer formed during the reaction. Comparison of the IV and DSC data shows that when the melting temperature of the polymer is higher than the maximum polymerization temperature, the intrinsic viscosity is notably higher. The melting temperatures of PA-10,T (327 °C), 50:50 10,T:6,T (324 °C) and 50:50 12,T:6,T (328 °C) are substantially higher than the final reaction temperature of 315 °C. These polymers also have the highest intrinsic viscosities (1.68, 1.68, and 2.17) and molecular weights (19,700, 19,700, and 27,000). Comparison of a molten (PA-12,T − Tm = 295 °C) and crystallized polymer (50:50 PA-12,T-co-6,T − Tm = 328 °C) shows a near doubling of intrinsic viscosity from 1.14 to 2.14 dL/g. This behavior is presumed to be due to solid state polymerization that occurs after the crystallization takes place within the reactor, a well-known phenomenon in nylon and polyester synthesis. Crystallization of polymer from the reaction increases the concentration of reactive groups in the melt and will drive the polymerization to higher conversions relative to a fully molten sample under the same polymerization conditions.

Despite the M_n differences discussed above, the copolymers could all be compression molded into tough, flexible films. This indicates that all copolymers were obtained with molecular weights above the critical value needed for good cumulative interactions and chain entanglement; thus, molecular weight variation effects in the obtained results are considered negligible. It is noteworthy to mention that the compression molding of 50:50 PA-12,T-co-6,T (the highest M_n) was the most difficult, requiring a much higher temperature and pressure compared to the other copolymers. Semi-aromatic polyamides are known to have markedly higher melt viscosities than all-aliphatic polyamides, and an IV of 2.16 ($M_n \sim 27{,}000$) may be approaching the upper limit with regard to processability of these materials.

3.2. ^{13}C NMR spectroscopy

High resolution NMR spectroscopy was used to determine copolymer composition and comonomer distribution. The ^{13}C NMR spectrum for PA-12,T is shown in Fig. 3. NMR spectra of the PA-10,T (12,T), 6,T copolymers showed multiple peaks for carbon atoms 1, 2, 3, and 4. Fig. 4 shows expanded regions of the α-amide carbon (4) and substituted aromatic carbon (2) of the related PA-12,T, PA-6,T copolymers. Slight variations in sample viscosity and solvent caused small peak shift changes; therefore peaks were aligned based on the α-amide carbon. The α-amide carbon (4) shows two distinct peaks representing the fraction of PA-12,T and PA-6,T in the copolymers. Their peak heights were found to correspond to the monomer feed ratios. Note that samples were prepared in wt-%, e.g., 50:50 wt-% is approximately 45:55 mol-% PA-12,T-co-6,T. This is significant since NMR spectral intensities reflect molar compositions.

In addition to the substituted aromatic carbon (2) peaks (Fig. 4, left) for PA-12,T and 6,T at 137.74 and 137.62 ppm respectively, two new peaks appear for all copolymers. The new peaks are due to the formation of PA-12,T–PA-6,T alternating sequences. This is further confirmed by comparing the 50:50 wt-% copolymer and a 50:50 wt-% mixed solution of the two homopolymers shown in Fig. 5. The physical mixture of the two homopolymers shows only two peaks for the substituted aromatic carbon, while the 50:50 copolymer has four peaks (Fig. 5, a and b). The new peaks are due to PA-12,T–PA-6,T alternating sequences and have identical peak heights. These data are consistent with completely random copolymers [15]. For example, for the 50:50 wt-% PA-12,T-co-6,T copolymers, the ratio of 12,T-12,T:12,T-6,T:6,T-6,T units is approximately 1:2:1, as expected for statistically random copolymers.

The relative peak intensities for varying amounts of PA-12,T, PA-6,T, and PA-12,T–PA-6,T sequences formed by varying the PA-6,T content of the copolymer from 15 to 50 wt-% are shown in Fig. 4 (left). At 15 wt-% PA-6,T (Fig. 4b), a small broad peak between the peaks for pure PA-6,T and the 12,T-6,T unit is seen. Comparison with the corresponding peak of the PA-12,T–PA-6,T sequence indicates little if any homo-sequences of PA-6,T exist at a 15 wt-% loading. At 30 wt-% PA-6,T, the peak due to PA-6,T homo-sequences increases, but the number of these sequences is still small compared to the 12,T and 12,T-6,T sequences. At 50 wt-% PA-6,T, the peak for PA-6,T homo-sequences is increased to approximately the same number as seen for 12,T homo-units and half that of 12,T-6,T sequences, what would be expected for a random melt condensation polymer. Since crystallinity is partially dependent on regularity of the polymer structure, the behavior of the substituted aromatic carbon should provide sequence information needed to help understand the eutectic melting behavior of the copolymer series as discussed below.

3.3. Differential scanning calorimetry

A series of second-heating DSC thermograms of PA-10,T-co-6,T (top trace) and 12,T-co-6,T (bottom trace) copolymers are shown in Fig. 6. Melting temperatures and enthalpies are plotted versus wt-% PA-6,T in Fig. 7. PA-10,T and PA-12,T homopolymers have melting temperatures of 315 and 292 °C, respectively. Copolymers showed

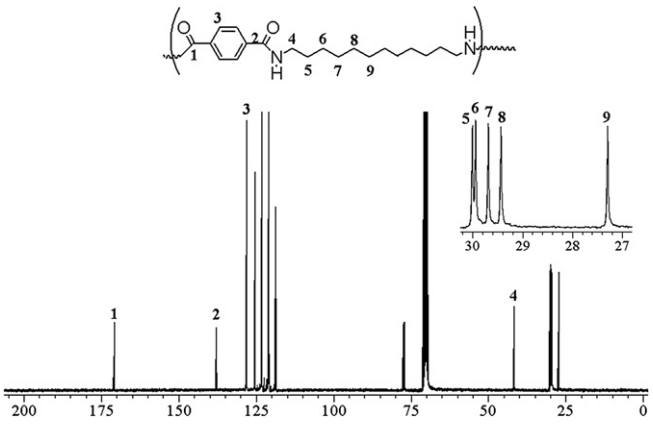

Fig. 3. ^{13}C NMR spectrum of PA-12,T.

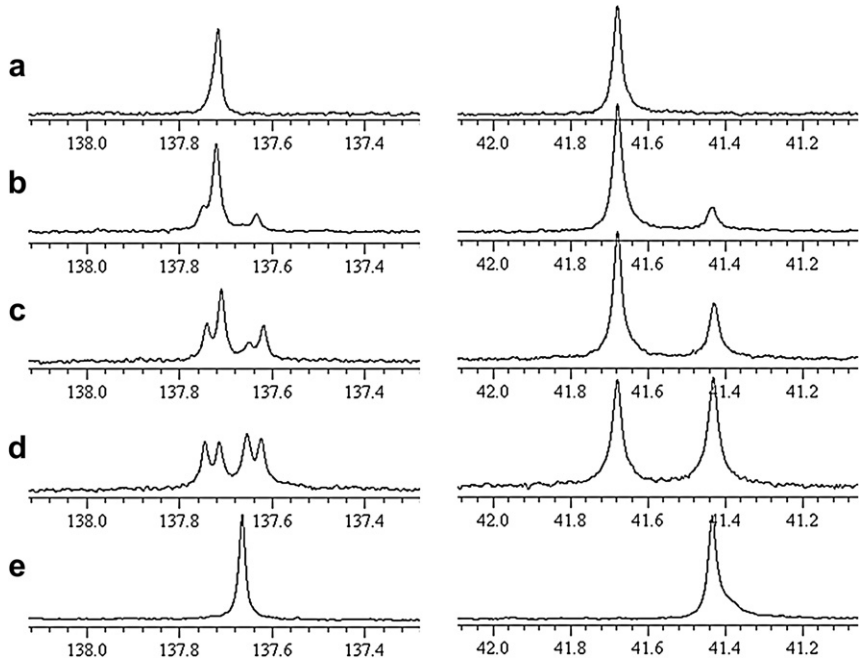

Fig. 4. Expanded ^{13}C NMR spectrum of substituted aromatic (left) and α-amide (right) carbon atoms of (a) PA-12,T, (b) 85:15 wt-% PA-12,T-co-6,T, (c) 70:30 wt-% PA-12,T-co-6,T, (d) 50:50 wt-% PA-12,T-co-6,T, and (e) PA-6,T.

a linear decrease in melting temperature with increasing PA-6,T comonomer content, with the lowest melting temperatures of 280 and 272 °C observed for PA-10,T-co-6,T and 12,T-co-6,T copolymers at ca. 30 wt-% PA-6,T, respectively. Similarly, melting enthalpies of both sets of copolymers displayed a linear decrease with increasing PA-6,T comonomer content. Melting enthalpies of PA-10,T-co-6,T and PA-12,T-co-6,T copolymers showed a minimum at 35 and 30 wt-% PA-6,T, respectively, decreasing from 70 to 24 J/g for PA-10,T-co-6,T and 60 to 26 J/g for PA-12,T-co-6,T copolymers. In addition, the melting endotherms of copolymers containing 30–40 wt-% PA-6,T were very broad compared to those of the respective homopolymers.

The data indicate that both PA-10,T and PA-12,T are not co-crystalline with PA-6,T. The 6 or 8 carbon difference in the diamine portion of the repeat unit of the former increases the length between amide units, and therefore inhibits entrance of the PA-6,T repeat unit into PA-10,T and 12,T crystal structures (and vice versa). The decreasing melting temperatures up to 30 wt-% PA-6,T are consistent with the formation of fewer and smaller or less perfect crystals, while the decrease in melting enthalpies is due to the overall decrease in the total crystallinity and crystal perfection as well. This implies that PA-6,T sequences up to 30 wt-% act as impurities, and inhibit the formation of PA-10,T or PA-12,T crystals. ^{13}C NMR spectroscopy has shown that with 15 wt-% PA-6,T, most PA-6,T units are statistically incorporated as PA-6,T–PA-12,T alternating units with no PA-6,T homo-sequences. This maximizes the number of irregularities along a given polymer chain, and therefore has a negative effect on crystal content as well as size and perfection of crystallites that do form. The broadening of the melting endotherms is also associated with a larger distribution of crystal size and perfection. Further support for this interpretation comes from the fact that compression molded films in this range of compositions have increased optical clarity with increasing PA-6,T content, consistent with the reduced crystallinity, and with 30 wt-% PA-6,T transparent materials are obtained.

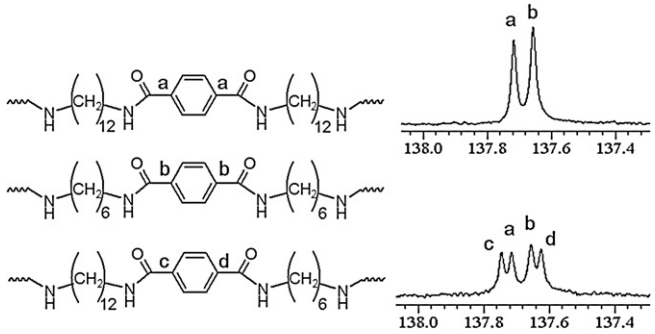

Fig. 5. Peak assignments of substituted aromatic ^{13}C NMR chemical shifts of the 50:50 PA-12,T-co-6,T copolymer (bottom spectra) and a 50:50 mixture (top spectra) of the two homopolymers.

The eutectic points for both PA-10,T-co-6,T and PA-12,T-co-6,T copolymer series were found at 30 wt-% PA-6,T. The depression of melting temperature and enthalpy may extend to lower values and result in a totally amorphous composition if 1–2 wt-% increments were used in the vicinity of the eutectic point. Increasing PA-6,T comonomer content above 30 wt-%, increased the melting temperature in a manner that was largely independent of which comonomer was present, that of PA-10,T or 12,T. NMR results indicated that, at 30 wt-% and higher PA-6,T content, longer PA-6,T sequences start being formed. The crystalline melting temperature of the PA-6,T homopolymer is 372 °C, and the homo-6,T crystallites may have reduced size and perfection that determine the melting point values. That is, on increasing above 30 wt-% 6-T content, the PA-10,T and 12,T homo-sequences and alternating sequences act as defects to the formation of PA-6,T crystals. This effect is reduced as the amount of PA-6,T comonomer was increased further. Melting temperatures of PA-10,T, 6,T and PA-12,T-co-6,T copolymers increased from 272 and 280 at 30 wt-% PA-6,T to 325 °C and 320 °C at 60 wt-% PA-6,T, respectively. The fact that an almost identical plot of the melting temperatures is seen for both copolymer series further confirms that formation of PA-6,T crystallites is the controlling factor in the solid polymers. In addition, melting

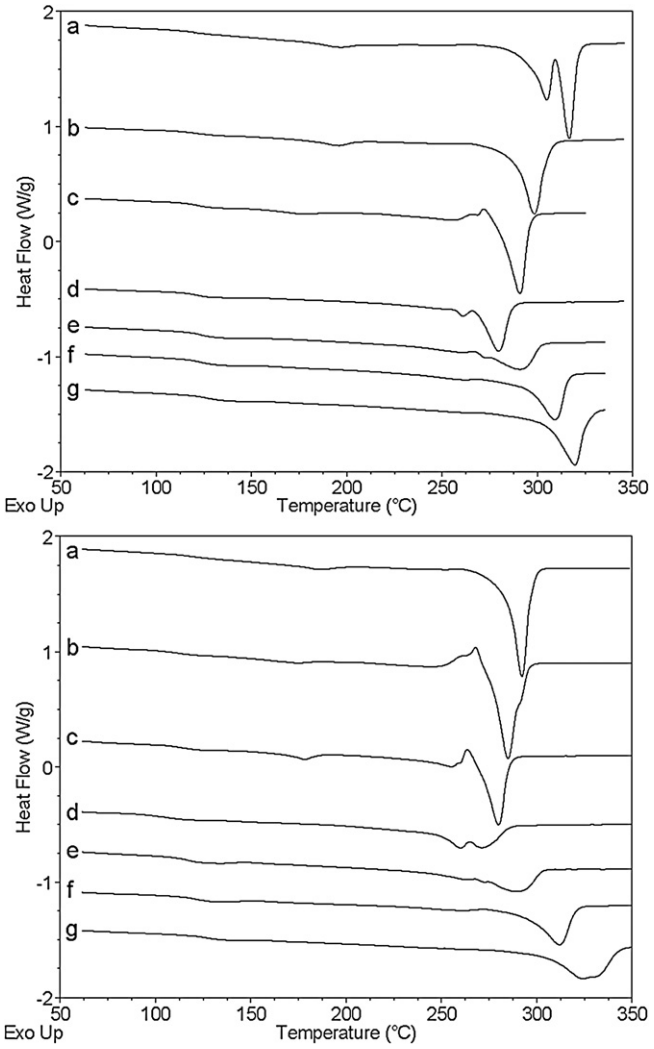

Fig. 6. Second-heating DSC thermographs of PA-10,T (top) and PA-12,T (bottom) containing 0 (a), 10 (b), 20 (c), 30 (d), 40 (e), 50 (f), and 60 (g) wt-% PA-6,T.

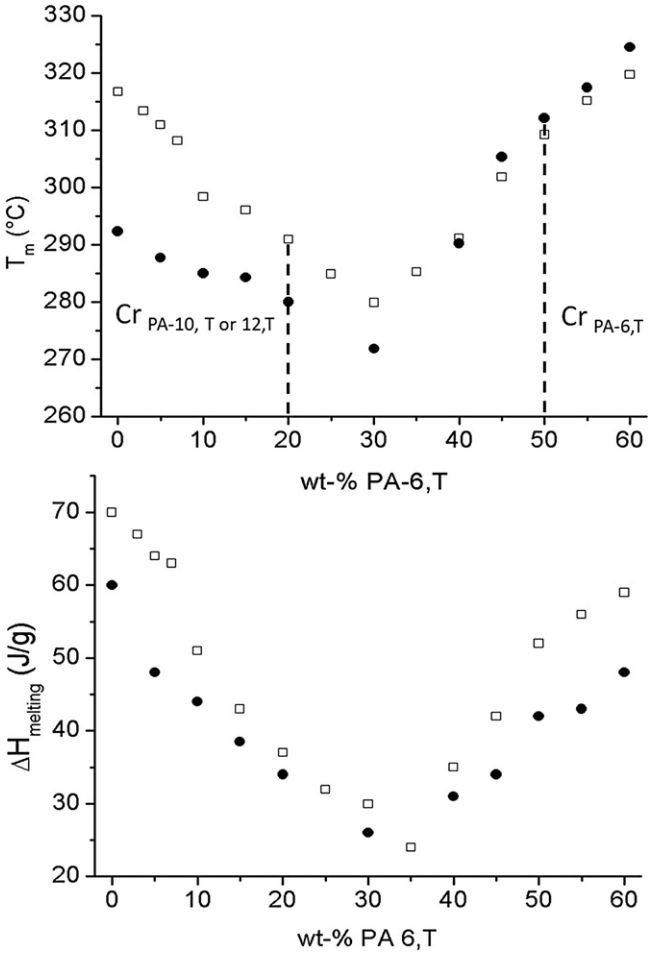

Fig. 7. Second-heating DSC melting temperatures (upper plot) and enthalpies (lower plot) of PA-10,T (□) and PA-12,T (●) versus wt-% PA-6,T. Labeled regions of crystal type are identified in Section 3.4.

enthalpies showed a corresponding increase with increasing PA-6,T content greater than 35 wt-%.

Copolymers exceeding 60 wt-% PA-6,T displayed phase separation, producing crystalline domains having melting points exceeding 350 °C. Since PA-6,T homopolymer has a melting point of 370 °C, the separated phase consists mostly of 6,T homo-sequences. The degree of phase separation was found to be affected by the thermal history of the polymer. For example, compression molding of the 40:60 10,T-co-6,T copolymer produced a film with different regions of clarity, similar to a stained glass pattern. Fig. 8 shows first heating DSC thermographs of both relatively (a) opaque white and (b) clear yellow domains in the compression molded film; the two domains were physically cut from the film and analyzed separately. The white sections (a) of the blotchy film have a larger PA-6,T rich phase melting enthalpy compared to the clearer area (b) of the film. It appears that compression molding at 340 °C induces phase separation and/or annealing of this higher melting phase, resulting in the blotchiness of the film. To confirm the annealing of the higher melting phase, DSC annealing of the bulk reaction material at 340 °C was performed for 30 min and compared to a control sample (c) heated to 340 °C in the DSC and immediately air cooled. Heating scans after these thermal treatments are shown in Fig. 8. The annealed sample displayed a higher melting peak approximately five times larger than that of the un-annealed sample, confirming that phase separation and annealing are occurring during melt pressing of the 40:60 PA-10,T-co-6,T copolymers. Since there was no mixing during the reaction and the maximum temperature was 316 °C, this phase separation could be a result of the crystallization of PA-6,T rich phases during the polymerization reaction. If crystallization during the reaction occurs, the randomness of the resulting polymer would be directly affected, thus physically changing the microscopic composition and morphology of the multiphase system generated. Despite having such separated crystal domains, tie molecules and material flow during compression molding were apparently sufficient to allow formation of tough films.

3.4. WAXD

X-ray diffraction was used to further confirm crystal composition of PA-10,T-co-6,T and PA-12,T-co-6,T copolymers. Copolymers of PA-10,T with 0–60 wt-% PA-6,T are shown in Fig. 9. For brevity, WAXD trends of PA-12,T-co-6,T copolymers are omitted, but show similar diffraction patterns with increasing PA-6,T content. Diffraction patterns of PA-10,T and 12,T compression molded films display sharp diffraction peaks at approximately 19.5, 20.5 and 20° 2θ<GK>. Note that the PA-6,T diffraction pattern was obtained from a powder, whereas all others are from compression molded films. Three regions of diffraction patterns were observed as labeled on the phase diagram in Fig. 7:

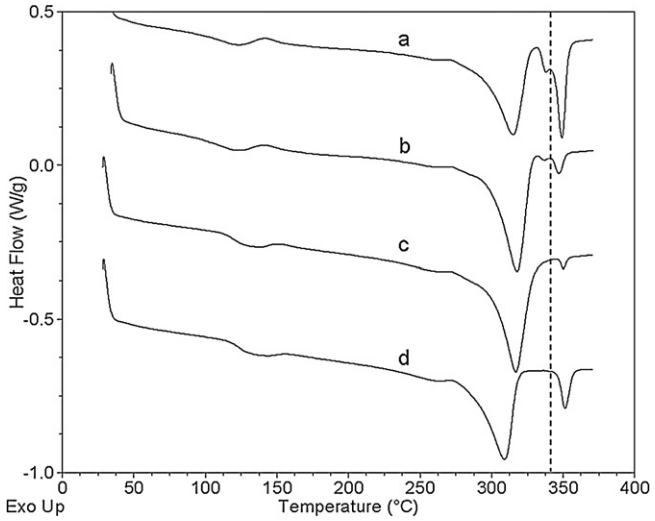

Fig. 8. DSC thermographs of white (a) and clear (b) regions of compression molded film, and un-annealed (c) and annealed (d) non-compression molded samples of the 40:60 wt-% PA-10,T-co-6,T copolymer (vertical line represents compression molding and DSC annealing temperature).

- 0–20 wt-% PA-6,T – Sharp diffraction peaks of PA-10,T broaden and their intensity decreases, falling into the amorphous halo when the PA-6,T content is increased to 20 wt-%. All diffraction peaks are consistent with PA-10,T homopolymer diffraction patterns. This confirms that the addition of low levels of PA-6,T disrupt PA-10,T crystal formation, and new types of crystals are not formed.
- 25–45 wt-% PA-6,T – No sharp diffraction peaks are observed between 25 and 45 wt-% PA-6,T, although DSC results show melting enthalpies between 24 and 30 J/g. The absence of sharp diffraction peaks is due to the low crystallinity of the samples and only broad amorphous scattering is observed. Increasing from 25 to 45 wt-%, the width of this broad diffraction increases from that of PA-10,T to PA-6,T. At 40–45 wt-% PA-6,T crystals are forming, but are still less intense than the amorphous phase halo. Due to the low crystallinity of these samples it cannot be said if PA-10,T and 6,T crystals are both formed in this intermediate range.
- 50–60 wt-% PA-6,T – The reappearance of sharp diffraction peaks is observed between 50 and 60 wt-% PA-6,T, giving peaks similar to those of the PA-6,T homopolymer synthesized by solution polymerization. This further confirms that, beyond the eutectic point, PA-6,T crystals are being formed.

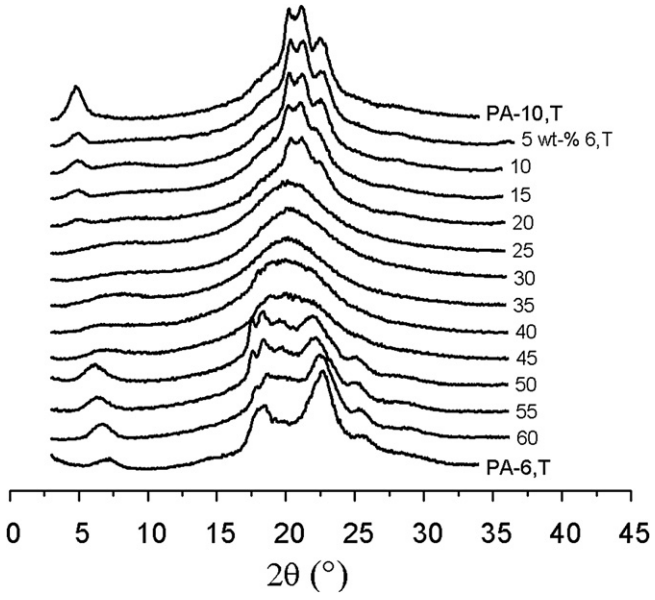

Fig. 9. X-ray diffraction patterns of PA-10,T-co-6,T copolymers.

X-ray diffraction patterns and DSC thermographs show good agreement, confirming the change of crystal type through the eutectic point. However, there is discrepancy between the two sets of data. PA-10,T copolymers with 15 and 45 wt-% PA-6,T have similar melting enthalpies (~43 J/g), while showing distinct differences in their diffraction patterns. It appears from the WAXD data, that crystallinity is higher in the former due to sharp diffractions peaks, while the latter displays only an amorphous halo. Since PA-6,T crystals have a higher amide density and thus a higher melting enthalpy, it can be inferred that the degree of crystallinity for the 45 wt-% PA-6,T copolymer is less, despite having the same melting enthalpy as the 15 wt-% copolymer.

3.5. Dynamic mechanical analysis

Change in the degree and type of crystallinity provided by the variation of comonomer sequence consequently impacts the composition of the amorphous phase and thermomechanical properties. Fig. 10 displays the tan δ of compression molded and annealed PA-10,T-co-6,T copolymer films obtained from dynamic mechanical analysis. All the DMA data, including the storage modulus at 75 and 200 °C and the maximum tan δ, are summarized in Table 2. The glass transition temperatures (T_g), as determined by the tan δ maximum for PA-10,T and PA-12,T were found to be 148 and 137 °C, respectively. PA-12,T has two additional flexible methylene groups per repeat unit when compared to PA-10,T, thus slightly decreasing the amide density and T_g. Both PA-10,T and 12,T with 15 wt-% PA-6,T display a small second transition at approximately 190 and 182 °C, respectively. This is consistent with the formation of a separate second phase. Although there exists no data in the literature describing the miscibility of these polymers, this work suggests that at 15 wt-% PA-6,T content, phase separation occurs resulting in this higher T_g transition. WAXD has shown that 6,T segments do not participate in homo-sequence crystallization at 15 wt-% PA-6,T. With this exclusion from the crystalline domain, the local content of PA-6,T in the amorphous domain increases upon crystallization of the 10,T or 12,T sequences. This results in a concentration and distribution of sequences that favor phase separation. At 30 and 50 wt-% PA-6,T, this shoulder disappears but an overall increase in T_g is observed. This slight increase in T_g is due to the increase of more rigid 6,T segments in the amorphous domain. Due to lack of crystallinity at these PA-6,T levels, the tan δ peak intensity is larger compared to the homopolymers.

Crystallites can act as reinforcing agents to tie the amorphous chains together in a physically crosslinked morphology; therefore, modulus should be somewhat proportional to the degree of crystallinity. Below T_g (75 °C), the amorphous chains are in a rigid state and this effect is not apparent. However, above T_g (200 °C) amorphous chains are mobile and the degree of crystallinity plays a dominant effect on the modulus of the material. Consistent with this interpretation, PA-10,T and 12,T homopolymers have the highest values of melting enthalpy and modulus at 200 °C. In relation to melting enthalpy, from 0 to 30 wt-% PA-6,T, the storage modulus above T_g decreases. This is consistent with the gradually decreasing degree of crystallinity. However, the melting enthalpy of the 50 wt-% PA-6,T copolymers significantly recovers from the eutectic point, while the storage modulus above T_g does not. For

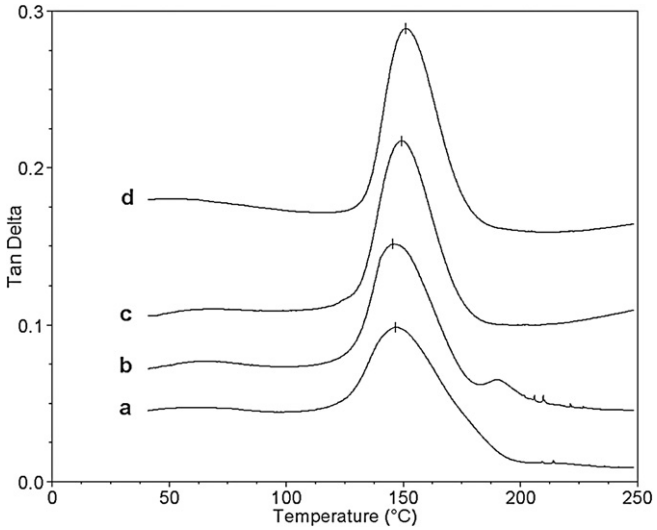

Fig. 10. DMA tan δ of PA-10,T (a) with 15 (b), 30 (c), and 50 (d) wt-% PA-6,T.

example, the 15:85 and 50:50 PA-12,T-co-6,T copolymers have similar melting enthalpies, but have a 20% difference in modulus value. Therefore, the rise in melting enthalpy from 30 to 50 wt-% PA-6,T is not solely due to the increase of the degree of crystallinity, but also corresponds to the change of crystal type from PA-12,T to PA-6,T. That is, the equilibrium heat of fusion of PA-6,T is higher than that of PA-12,T (10,T) because of the increased concentration of amide groups per gram of crystals. Therefore, comparing melting enthalpies to the left and the right side of the eutectic point does not properly describe relative degrees of crystallinity but is also related to other contributions to inter- and intramolecular interactions in these materials. This is in agreement with WAXD data as noted earlier, where the PA-10,T crystals at 15 wt-% PA-6,T were found to show sharper peaks than those for PA-6,T homopolymer crystals and the 50 wt-% PA-6,T sample.

4. Discussion

Copolyamide crystallization behavior is a result of the symmetry of amide distance and orientation of the comonomer repeat unit structure. For example, nylon 6,6-co-6,T copolymers exhibit co-crystalline (isomorphic) behavior because they are both A–A B–B, even–even monomers, and the distance between amide groups formed from adipic and terephthalic acids has only a 0.3 angstrom difference in length [5]. Therefore, they display an almost linear trend of melting temperature with increasing content of the PA-6,T comonomer. These data are shown in Fig. 11 with PA-12,T-co-6,T, PA-10,T-co-6,T and several other PA-6,T copolymers as a function of PA-6,T comonomer content.

Table 2
DMA storage modulus and maximum tan δ values plus DSC enthalpy values for PA-10,T-co-6,T and PA-12,T-co-6,T copolymers.

	E′ at 75 °C (MPa)	E′ at 200 °C (MPa)	tan δ_{max}	$\Delta H_{melting}$ (J/g)
PA-10,T	1800	470	148	70
15 wt-% PA-6,T	1890	330	146	43
30 wt-% PA-6,T	1850	260	149	30
50 wt-% PA-6,T	1880	260	149	52
PA-12,T	1820	450	137	60
15 wt-% PA-6,T	1690	360	140	38
30 wt-% PA-6,T	1729	240	142	26
50 wt-% PA-6,T	1810	280	144	42

All other PA-6,T copolymer units are not isomorphic, displaying a minimum melting temperature as a function of composition. Fig. 11 shows that the eutectic melting behaviors of these copolyamides are distinct in terms of the minima location and shape of the plot. For example, PA-12,T-co-6,T, PA-10,T-co-6,T copolymers display a smaller melting point depression with a minimum occurring at higher amounts of PA-6,T, compared to the nylon 6-co-6,T copolymers. At the eutectic point, the total decrease in melting temperature from nylon 6 homopolymer is 88 °C with 16 mol-% PA-6,T, while for PA-12,T-co-6,T and PA-10,T-co-6,T copolymers these values are only 20 °C at 34 mol-% and 35 °C at 37 mol-%, respectively. This implies that PA-6,T disrupts nylon 6 crystallinity to a greater extent than those of PA-10,T and PA-12,T. This behavior can be attributed to greater similarities in PA-10,T, 12,T, and 6,T repeat unit structures. These terephthalamide copolymers maintain a regular hydrogen bonding orientation and placement, and all have an even number of carbon atoms between amide bonds. Alternatively, PA-6 includes a reverse amide bond due to the head-to-tail linkage of the A–B structure with an odd number of carbon atoms between amide bonds. Therefore, addition of PA-6,T has a larger effect on the eutectic melting behavior of nylon 6 than 10,T or 12,T. The degree of the eutectic depression has been discussed for poly(ethylene terephthalate-co-p-benzoates) copolyesters [16]. Since there was a noticeably smaller drop in melting temperature at the eutectic point compared to poly(ethylene terephthalate-co-adipate) and poly(ethylene terephthalate-co-sebacate) it was concluded that the copolymers were partially isomorphous(or isodimorphic).

The effect of chain orientation can be understood by comparison with PA-6,I, 6,T copolymers. PA-6,I is amorphous due to its kinked chain. Its copolymers display no crystallinity up to 43 mol-% PA-6,T [17]. Both the amide bond length and chain orientation are affected by inclusion of the isophthalamide structure. The data show the PA-6,T crystals can have exceedingly low melting temperatures (<250 °C) in such copolymers [18], although the eutectic behavior of the fully terephthalamide polymers does not show such reduced melting points for the onset of PA-6,T crystallinity. For example, PA-10,T-co-6,T, and 12,T-co-6,T copolymers have respective lowest melting points of 281 and 270 °C despite having different lengths between amide bonds. Therefore, the symmetry of the aromatic substitution (meta versus para) and its effect on chain orientation and packing prevail over the distance between amide bonds, and this affects the eutectic melting temperature trends. Correspondingly, PA-4,T,

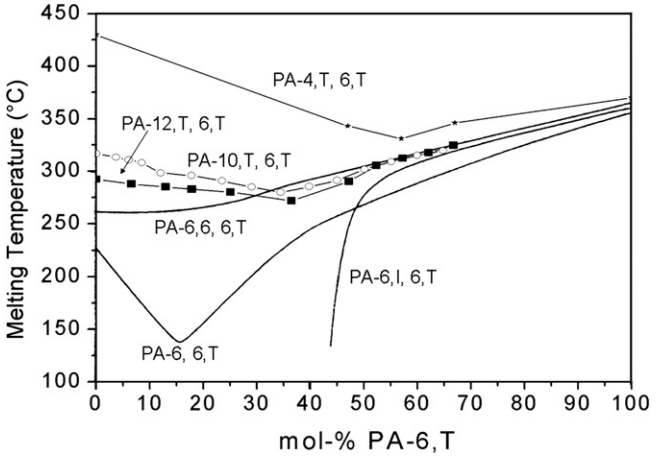

Fig. 11. PA-10,T(12,T)–6,T copolymer melting data overlaid with several additional PA-6,T copolymers versus mol-% PA-6,T.

6,T terephthalamide copolymers display a similar shape (Fig. 11) as PA-10,T-co-6,T and 12,T-co-6,T, although the composition at which the eutectic point occurs is reversed because PA-6,T is the lower melting component here. Distinct from the isophthalamide copolymers, terephthalamide sequences maintain a symmetrical chain orientation in both homo and alternating segments. Their unique melting point trends are associated with the ability of alternating units to crystallize or participate in homopolymer crystal formation in the eutectic well. Thus, they do not display a large reduction in the melting point of PA-6,T crystals as is seen for PA-6,I, 6,T copolymers.

A final observation relates the isomorphic PA-6,6, 6,T copolymers with isodimorphic PA-10,T-co-6,T and 12,T-co-6,T copolymers since their melting behaviors at compositions greater than 50 mol-% PA-6,T are similar. In general, the melting temperatures of isomorphic copolymers are a function of crystal composition, while isodimorphic crystalline melting is a function of crystal amount and size. Consequently, the density of PA-6,6, 6,T isomorphic copolyamides were found to rise with increasing PA-6,T content [5], whereas the crystallinity of PA-10,T(12,T), 6,T copolymers was shown to fall and then rise with increasing PA-6,T content. Despite these differences in behavior, PA-6,6, 6,T and PA-10,T(12,T)–6,T copolymers exceeding 50 mol-% PA-6,T have different crystalline properties, yet have the same melting temperature.

5. Conclusions

Melt condensation polymerization of PA-10,T and 12,T with PA-6,T comonomer has been demonstrated to produce statistical copolymers. The ^{13}C chemical shift of the substituted aromatic carbon is sensitive to the comonomer connectivity at different compositions, providing key chemical information in describing the physical changes of the above mentioned copolymers. It was found that at 15 and 30 wt-% PA-6,T, few pure PA-6,T sequences exist, and the majority of the PA-6,T comonomer is found in PA-10,T (or 12,T) –PA-6,T alternating sequences. Since the comonomers are not co-crystalline, PA-10,T (or 12,T) –PA-6,T alternating units act as impurities that inhibit the formation of PA-10,T or (12,T) crystals. This is supported by a decrease in melting temperature and enthalpy by DSC, the loss of sharp x-ray diffraction peaks up to 30 wt-% PA-6,T, and the increased clarity of compression molded films. However, PA-6,T content greater than 30 wt-% increases the melting temperature of the corresponding copolymer in a manner independent of the comonomer composition. Past the eutectic point, pure 6,T sequences become sufficiently abundant to crystallize alone. NMR analysis confirmed increases in PA-6,T homosequences above 50 wt-% PA-6,T. X-ray diffraction in this composition range also displayed sharp diffraction peaks that correspond to PA-6,T crystals.

It has been demonstrated that melting temperatures and the degree of crystallinity can be tuned by changing the amount of PA-6,T comonomer in PA-10,T-co-6,T and PA-12,T-co-6,T copolymers. These properties affect the processability, degree of crystallinity and optical clarity of the resulting copolymers, while maintaining higher glass transition temperatures than pure aliphatic polyamides.

Acknowledgments

The authors would like to thank Dr. W.L. Jarrett for ^{13}C NMR help with interpretation, Dr. Kenneth Mauritz for the use of his DMA equipment, and Ascend Performance Materials for providing funding and starting materials, and the use of their Parr equipment.

References

[1] Kohan MI. Nylon plastics handbook. New York: Carl Hanser Verlag; 1995. p. 372–4 and 594–9.
[2] Morgan PW, Kwolek SL. Macromolecules 1975;8(2):104–11.
[3] Shashoua VE, Eareckson WM. Journal of Polymer Science 1959;40:343–58.
[4] Kaitian X, Jarrett WL, Mathias LJ. Polymer Preprints 2005;46(1):789–90.
[5] Edgar OB, Hill R. Journal of Polymer Science 1952;8:1–22.
[6] Yu AJ, Evans RD. Journal of Polymer Science 1960;42:249–57.
[7] Harveym ED, Hybart FJ. Polymer 1971;12:711–6.
[8] Gaymans RJ, Aalto S, Maurer FHJ. Journal of Polymer Science, Part A: Polymer Chemistry 1989;27:423–30.
[9] Togashsi O, Umetsu H, Iwamoto M. European patent 0448221; 1991.
[10] Wunderlich B. Macromolecular physics. New York: Academic Press; 1973. p. 147–61.
[11] Liu H, Yang G, He A, Wu M. Journal of Applied Polymer Science 2004;94:819–26.
[12] Rulkens R, Crombach RCB. United States patent 6,747,120; 2004.
[13] Solomon OF, Ciuta IZ. Journal of Applied Polymer Science 1962;6:683.
[14] Novitsky TF, Lange CA, Mathias LJ, Osborn S, Manning S, Ayotte R. Journal of Applied Polymer Science 2010;116(6):3388–95.
[15] Aerdts AM, Eersels KLL, Groeninckx G. Macromolecules 1996;29:1041–5.
[16] Meesiri W, Menczel J, Gaur U, Wunderlich B. Journal of Polymer Science, Part B: Polymer Physics 1982;20:719–28.
[17] Blaschke F, Ludwig W. United States patent 3,382,216; 1968.
[18] Lum FG, Carlston EF. Industrial Engineering and Chemistry 1952;44 (7):1595–600.